



ELSEVIER

Colloids and Surfaces A: Physicochem. Eng. Aspects 220 (2003) 9–27

COLLOIDS  
AND  
SURFACES

A

www.elsevier.com/locate/colsurfa

# Effects of petroleum resins on asphaltene aggregation and water-in-oil emulsion formation

P. Matthew Spiecker<sup>a</sup>, Keith L. Gawrys<sup>b</sup>, Chad B. Trail<sup>c</sup>,  
Peter K. Kilpatrick<sup>b,\*</sup>

<sup>a</sup> ExxonMobil Upstream Research Company, Houston, TX 77027, USA

<sup>b</sup> Department of Chemical Engineering, North Carolina State University, Raleigh, NC 27695, USA

<sup>c</sup> University of Kentucky, Lexington, KY 40506, USA

Received 22 July 2002; accepted 30 December 2002

## Abstract

Asphaltenes from four crude oils were fractionated by precipitation in mixtures of heptane and toluene. Solubility profiles generated in the presence of resins (1:1 mass ratio) indicated the onset of asphaltene precipitation occurred at lower toluene volume fractions (0.1–0.2) than without resins. Small-angle neutron scattering (SANS) was performed on solutions of asphaltene fractions in mixtures of heptane and toluene with added resins to determine aggregate sizes. Water-in-oil emulsions of asphaltene–resin solutions were prepared and separated by a centrifuge method to determine the vol.% water resolved. In general, the addition of resins to asphaltenes reduced the aggregate size by disrupting the  $\pi$ – $\pi$  and polar bonding interactions between asphaltene monomers. Interaction of resins with asphaltenic aggregates rendered the aggregates less interfacially active and thus reduced emulsion stability. The smallest aggregate sizes observed and the weakest emulsion stability at high resin to asphaltene (R/A) ratios presumably corresponded to asphaltenic monomers or small oligomers strongly interacting with resin molecules. It was often observed that, in the absence of resins, the more polar or higher molecular weight asphaltenes were insoluble in solutions of heptane and toluene. The addition of resins dissolved these insolubles and aggregate size by SANS increased until the solubility limit was reached. This corresponded approximately to the point of maximum emulsion stability. Asphaltene chemistry plays a vital role in dictating emulsion stability. The most polar species typically required significantly higher resin concentrations to disrupt asphaltene interactions and completely destabilize emulsions. Aggregation and film formation are likely driven by polar heteroatom interactions, such as hydrogen bonding, which allow asphaltenes to absorb, consolidate, and form cohesive films at the oil–water interface.

© 2003 Elsevier Science B.V. All rights reserved.

**Keywords:** Asphaltenes; Resins; Emulsion stability; Small-angle neutron scattering

## 1. Introduction

Emulsion challenges during petroleum recovery have been attributed to colloidal aggregation of

\* Corresponding author. Tel.: +1-919-515-7121; fax: +1-919-515-3465.

E-mail address: peter-k@eos.ncsu.edu (P.K. Kilpatrick).

asphaltenes and waxes [1–6]. Many early studies were performed on the film forming and emulsifying behavior of crude oil–water systems [1,7–15]. These and later studies often pointed to the asphaltenic constituents in crude oil as being responsible for film formation and stabilization [10,11,16,17].

Asphaltenes, or *n*-heptane insolubles and toluene solubles, are the most refractory compounds present in crude oil and are generally distinguished by a fused aromatic core with polar heteroatom functionality [18,19]. Studies indicate the presence of carboxylic acids, carbonyls, phenols, pyrroles and pyridinic functional groups capable of accepting or donating protons [20–24]. Vapor pressure osmometry measurements suggest number average molecular weights range from approximately 800 to 3000 Da [25–32]. Even lower asphaltene molecular weights are observed in hot, polar solvents suggesting that aggregates formed through stacking interactions between asphaltene monomers. The most plausible mechanisms of asphaltene aggregation involve  $\pi$ – $\pi$  overlap between aromatic sheets, hydrogen bonding between functional groups and other charge transfer interactions.

Small-angle neutron scattering (SANS) has been applied to probe solvent and temperature effects on asphaltene aggregation [33–44]. Proper analysis of the scattering intensity curves can provide aggregate size, shape, molecular weight, and fractal dimension. Asphaltenic aggregates are comprised of cofacial stacks of planar, fused aromatic ring moieties connected by aliphatic chains and rings. Recent structural and molecular modeling seem to confirm the so-called ‘archipelago’ model of asphaltenes, as opposed to the more widely implied and invoked ‘island’ model [45]. In the ‘archipelago’ model, individual asphaltene monomers are comprised of aromatic and fused aromatic ring moieties, some with polar functional groups, connected to each other by aliphatic polymethylene chains and rings that likely contain some sulfide and carbonyl functional groups (see Fig. 1). Asphaltenic aggregates have been modeled as mono- and polydisperse spheres [35,46], flat disks [37,47,48], and prolate cylinders [38]. Asphaltene polydispersity, however, makes the pre-

cise shape difficult to discriminate. With the archipelago-like structure of Fig. 1, it seems probable that asphaltenic aggregates possess a porous reticulated microstructure.

While the effects of temperature, solvent aromaticity, and polarity have received much attention, the solvation of asphaltene aggregates by resins has not been fully explored. What we mean here by the expression ‘solvation’ is the strong local interaction of asphaltenic aggregates by resin molecules, a phenomenon referred to in previous studies by the curious term ‘peptized’; we do not mean by solvation the ‘swelling’ of asphaltenic aggregates, although as we show in a subsequent publication, resins definitely fill in solvent voids in asphaltenic aggregates created by the reticulated structure of asphaltenes. Espinat et al. measured neutron and X-ray scattering intensities from asphaltenic aggregates in several solvents, at low and high temperatures and with added resins [37]. The scattering curves were fit using a thin disc form factor model. In toluene, 2 wt.% Boscan asphaltene solutions formed larger aggregates at room temperature (234 Å diameter) than at 76 °C (175 Å). At room temperature, aggregate sizes were two to four times smaller in high polarity solvents such as pyridine and tetrahydrofuran than in benzene. They also found that resin–asphaltene ratios of 2:1 by mass reduced the scattering intensity at low *Q* suggesting the formation of smaller aggregates. However, the effect of resin solvation on asphaltene aggregate size was not explicitly reported. Bardon et al. observed resin solvation of Safaniya asphaltenes using SANS and SAXS [47]. Weight average molecular weights of 2 wt.% asphaltene solutions in toluene with R/A ratios of 2, 4, and 8:1 were reduced by factors of 2.6, 4.6, and 7.5, respectively.

Previously [44,49] we examined the aggregation and emulsion stabilizing behavior of asphaltenes and their more and less soluble fractions in mixtures of heptane and toluene (so-called ‘heptol’). Gravimetric solubility measurements indicated that asphaltenes start to precipitate at concentrations between 45 and 52% (v/v) toluene in heptol. Precipitation concentrated the most aromatic and polar constituents as measured by H/C ratio and nitrogen content. In addition,

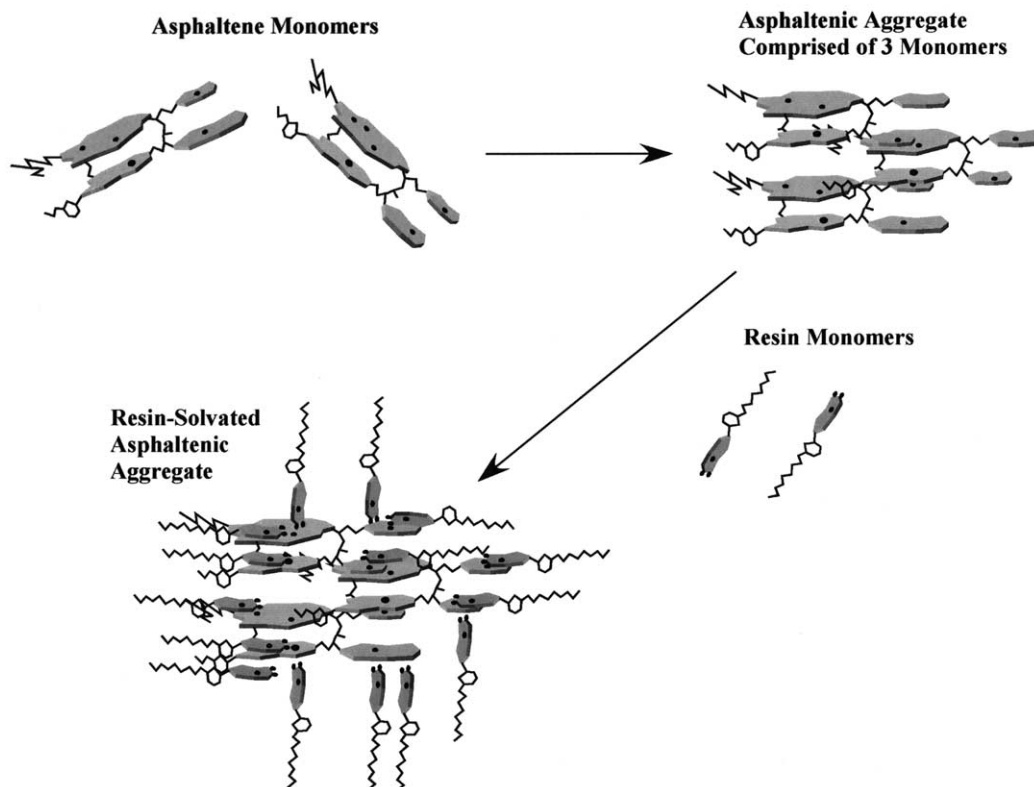


Fig. 1. Schematic illustration of archipelago model of asphaltene monomers, asphaltenic aggregate in absence of resins, and asphaltenic aggregate in presence of resins.

SANS indicated that the less soluble fraction formed the largest aggregates in heptol while the more soluble fraction formed considerably smaller aggregates. Asphaltenes and their various sub-fractions are well known to stabilize water-in-oil emulsions near the point of incipient flocculation [50]. The degree of aggregation and proximity to the solubility limit governs the stability of emulsions prepared in heptol.

In this study, we have taken another step towards understanding the mechanisms of asphaltene aggregation and emulsion formation in petroleum and petroleum-derived systems through the addition of solvating molecules. Crude oils are usually characterized by SARA fractionation where asphaltenes are removed by precipitation with a paraffinic solvent and the deasphalted oil (DAO or maltenes) is separated into saturates, aromatics and resins by chromatographic separa-

tion [51–55]. Resins are the most polar and aromatic species present in deasphalted oil and, it has been suggested, contribute to the enhanced solubility of asphaltenes in crude oil by solvating the polar and aromatic portions of the asphaltenic molecules and aggregates [25,56,57]. The solubility of asphaltenes in crude oil is mediated largely by resin solvation and thus resins play a critical role in precipitation, and emulsion stabilization phenomena [37,40,58–60]. Resins, although quite surface-active, have not been found to stabilize significantly water-in-oil emulsions by themselves in model systems, a fact that mitigates somewhat against the notion that resins and asphaltenes form a simple continuum of molecular structures and functions [61,62]. However, the presence of resins in solution can destabilize emulsions via asphaltene solvation and/or replacement at the oil–water interface [62–66].

Here we probe the effects of resins on asphaltene aggregation and emulsion formation. Aggregation is likely controlled by the ability of asphaltene monomers to interact through aromatic and polar forces. By fractionating asphaltenes into solubility classes, the most polar and aromatic species can be concentrated. The effectiveness of solvating resins on these more and less soluble asphaltenes aids in elucidating the mechanisms of colloid formation and emulsion stabilization in petroleum derived fluids.

## 2. Experimental

### 2.1. Asphaltene precipitation and fractionation

Asphaltenes were precipitated from four crude oils in a 40:1 excess of *n*-heptane. The crude oils were obtained from several locations around the world: B6 and Hondo (off-shore California), Arab Heavy (Safaniya), and Canadon Seco (Argentina). For brevity the following abbreviations will be used to describe the asphaltenes generated from Hondo, Arab Heavy, and Canadon Seco crude oils, respectively: HO, AH, and CS. These crude oils are asphaltene rich and vary in viscosity, resin content and asphaltene H/C ratio. Basic crude oil and asphaltene properties can be found in Table 1. Resin content was determined by sequential elution chromatography (discussed in the next section), H/C ratios were calculated from combustion elemental analysis (Perkin Elmer Series II CHNSO), and viscosity measurements were performed on a Rheometrics Dynamic Stress Rheometer with concentric cylinder geometry. Asphaltenes precipitated from the crude oils were separated into more and less soluble fractions by

dissolving in toluene and inducing partial precipitation through heptane addition. Enough heptane was added during fractionation to generate approximately 33% (w/w) insoluble asphaltenes from a 0.75% (w/v) asphaltene solution in toluene. All solvents were HPLC grade and obtained from Fisher Scientific. Details of the precipitation and fractionation procedures can be found in another publication [44]. A summary of the elemental composition of the asphaltene fractions is provided in Table 2.

### 2.2. SARA fractionation

Petroleum resins were isolated via the SARA technique where DAO is charged to silica gel and extracted with solvents of increasing polarity [51–53,67]. After a two stage filtration to ensure complete removal of the asphaltenes, the heptane-diluted crude oil was rotary evaporated until dry. The DAO was dissolved in methylene chloride (Fisher-HPLC grade) and adsorbed to activated silica gel (Chromatographic silica gel, 35–60 mesh, Fisher). Silica gel activation proceeded under vacuum at 120 °C for 48 h. The silica gel–DAO slurry was shaken for 24 h then rotary evaporated until dry and placed in a nitrogen flushed vacuum oven at 50 °C for 24 h.

Chromatography columns (2 × 100 cm with 250 ml solvent reservoir) were initially filled with a mixture of 68:32 heptane–toluene (v/v). Clean activated silica gel was added until the depth reached ~20 cm. Finally, silica gel with adsorbed DAO was transferred to the column until full. A solvent mixture containing 68% (v/v) heptane and 32% (v/v) toluene eluted saturates, mono-, di-, and triaromatics from the silica gel. Once the saturates and aromatics were extracted, a more polar

Table 1  
Crude oil properties

Crude	wt.% Asph	R/A ratio	H/C Asph	Viscosity (cP) 100°F
AH	6.7	1.12	1.14	33.8
B6	13.1	0.92	1.24	2030
CS	7.5	1.19	1.11	70
HO	14.8	1.39	1.29	363

Table 2  
Asphaltene fraction composition in wt.%, except H/C

Asphaltene	H/C			Nitrogen			Sulfur		
	Sol	Whole	Ppt	Sol	Whole	Ppt	Sol	Whole	Ppt
AH	1.17	1.14	1.13	0.92	1.02	1.08	8.06	8.32	7.66
B6	1.30	1.24	1.22	1.81	1.87	1.93	7.25	6.68	6.33
CS	1.12	1.11	1.09	1.32	1.32	1.39	0.52	0.52	0.48
HO	1.30	1.29	1.24	1.95	1.99	2.11	8.42	8.53	8.48

solvent (40:30:30 acetone:toluene:methylene chloride) was applied to elute the resins. The resin-solvent mixture was filtered to remove any silica gel fines and rotary evaporated until dry. The resins were transferred to jars and placed in a nitrogen flushed vacuum oven at 60 °C for 48 h or until completely dry. Combustion elemental analyses of the resins appear in Table 3.

### 2.3. Asphaltene and resin solubility

The solubility of asphaltenes and their sub-fractions were determined in heptol with added resins. Resins from the crude oil were only added to their complementary asphaltenes. Solubility profiles of the asphaltenes without resins were obtained in another study [44] and will be used for comparison. Resin–asphaltene solutions were prepared in various mixtures of heptane and toluene. The asphaltene concentration was 0.75% w/v (~ 1 wt.%) in 15 mL solvent and the resin–asphaltene ratio was 1:1 by mass. Resins and asphaltenes were dissolved together in toluene and allowed to shake for 12 h prior to heptane addition. After an additional 12 h, the solutions were vacuum filtered through 1.5 µm Whatman 934 AH filter paper to collect precipitates and rinsed with 7.5 ml of heptol

Table 3  
Resin composition in wt.%, except H/C (O by difference)

Resin source	H/C	N	S	O
AH	1.31	0.81	6.49	1.53
B6	1.51	1.48	6.91	1.98
CS	1.39	1.52	0.88	2.77
HO	1.51			

at the same toluene volume fraction. To ensure all of the resins were removed, the precipitate was rinsed with neat heptane prior to dissolution in methylene chloride. The % precipitated was determined from the mass ratio of precipitated asphaltenes to the original asphaltene mass.

### 2.4. Small-angle neutron scattering

Neutron scattering of asphaltenic aggregates solvated by resins was performed on the NG7 and NG1 small angle spectrometers at the NIST Center for Neutron Research (Gaithersburg, MD) or on the Small Angle Neutron Diffractometer (SAND) at Argonne National Laboratory (IPNS, Argonne, IL). Samples were measured in cylindrical quartz cells (NSG Precision Cells) with a path length of 5 mm (all NG7 samples) or 2 mm (all SAND samples).

Mixtures of asphaltenes and resins were prepared at resin:asphaltene (R/A) ratios between 0.25:1 and 10:1. Asphaltene solutions (1 wt.%) were prepared in perdeuterated heptane and toluene solutions (CDN Isotopes, Canada) and studied at 25 and 80 °C. Scattering intensity versus scattering angle ( $I(Q)$  vs.  $Q$ ) data were fit to Lorentzian line shapes using a non-linear least squares regression to determine the aggregate correlation lengths. Following Ornstein–Zernike formalism the scattering intensity,  $I$ , can be related to the scattering vector,  $Q$ , by:

$$I(Q) = \frac{I_0}{1 + (Q\xi)^2} \quad (1)$$

where  $\xi$  is the correlation length,  $I_0$  is the scattering intensity at  $Q = 0$  [42,68]. In some asphaltene

systems, a Porod upturn was observed at low  $Q$  where the scattering intensity increased monotonically with decreasing  $Q$ . Furthermore, incoherent scattering of all nuclei in the solvent and solute with non-zero spin was manifested in the scattering curves at large  $Q$  values (typically  $Q > 0.1$ ) as an isotropic background signal. The  $Q$  values that marked the transition from the Guinier regime to the Porod or incoherent scattering regimes were determined from inflection points in the scattering curves. The Lorentzian line shape described in Eq. (1) was applied over the intermediate range of  $Q$  values between the inflection points.

In the absence of a significant low  $Q$  upturn, Guinier analysis was also performed to calculate the radius of gyration,  $R_g$ , which is defined as the mean squared distance from the center of gravity of the scatterer. The Guinier approximation applies to aggregates in dilute solution and is strictly valid in the low  $Q$  range where  $QR_g$  is less than 1. The Guinier approximation has the form:

$$I(Q) = I_0 e^{(-Q^2 R_g^2/3)} \quad (2)$$

where

$$I_0 = N_p V_p (\Delta\rho)^2 \quad (3)$$

and  $N_p$  is the number of scatterers,  $V_p$  is the scatterer volume, and  $\Delta\rho^2$  is the coherent scattering contrast between the solvent and solute. Given that elemental compositions of the asphaltenes and resins are available, it is possible to calculate the scattering contrast terms and subsequently, the weight-average molecular weight of the aggregates in the Guinier regime. These analyses will be addressed in a future paper.

Comparing the analytical form of the Guinier approximation and Lorentzian lineshapes predicts that  $R_g$  should be proportional to  $\xi$  by a scale factor of  $\sqrt{3}$  (or  $\sim 1.73$ ). A comparison of the  $R_g$  and  $\xi$  values obtained from experiments on asphaltene and resin mixtures in heptol provides the relation  $R_g = 1.71\xi$ . This suggests that Guinier analysis and Lorentzian fits are equally suitable for extracting relevant aggregation behavior from scattering curves. Further details concerning the SANS instruments, experimental conditions, and data analysis methods are provided elsewhere [44].

## 2.5. Resin–asphaltene emulsions

Water-in-oil emulsions were prepared by homogenizing water and model oil solutions containing asphaltenes and resins. Asphaltenes and resins were dissolved together in toluene for approximately 12 h followed by heptane addition. A 4 mL aliquot of this solution with an asphaltene concentration of 0.37% w/v ( $\sim 0.5\%$  w/w) was homogenized with a 6 mL aliquot of deionized water. A Virtis Virtishear Cyclone I.Q. homogenizer with a 6 mm rotor–stator emulsion generator assembly was lowered into the oil–water system and run at 15 000 rpm for 3 min.

After aging 24 h, the emulsions were centrifuged for 1 h at 15 000 rpm. The stability of the emulsions was calculated from the volume of water resolved:

$$\% \text{ Water resolved} = \frac{\text{Volume resolved}}{\text{Initial volume}} \times 100 \quad (4)$$

Complete details on solution preparation and homogenization can be found elsewhere [49].

## 3. Results and discussion

### 3.1. Asphaltene–resin solubility

The effect of adding resins (1:1 mass ratio) on asphaltene solubility is shown in Fig. 2(a–d). The half filled markers represent solubility data determined for asphaltenes in neat heptol while the filled markers represent asphaltene solubility with resins. As mentioned before, the solubility limits of the whole asphaltene fractions were approximately 50% toluene. The more soluble fraction or ‘Soluble’ asphaltenes precipitated at toluene volume fractions between 0.3 and 0.4 while the less soluble or ‘Precipitate’ asphaltenes precipitated at considerably higher aromaticity (0.6–0.8). This indicates that the Soluble fraction cooperatively solvates the Precipitate fraction in solution.

The process of fractionation generated unique asphaltene classes distinguished by their solubility behavior. The Precipitate fractions were characterized by higher aromaticity, polarity, molecular

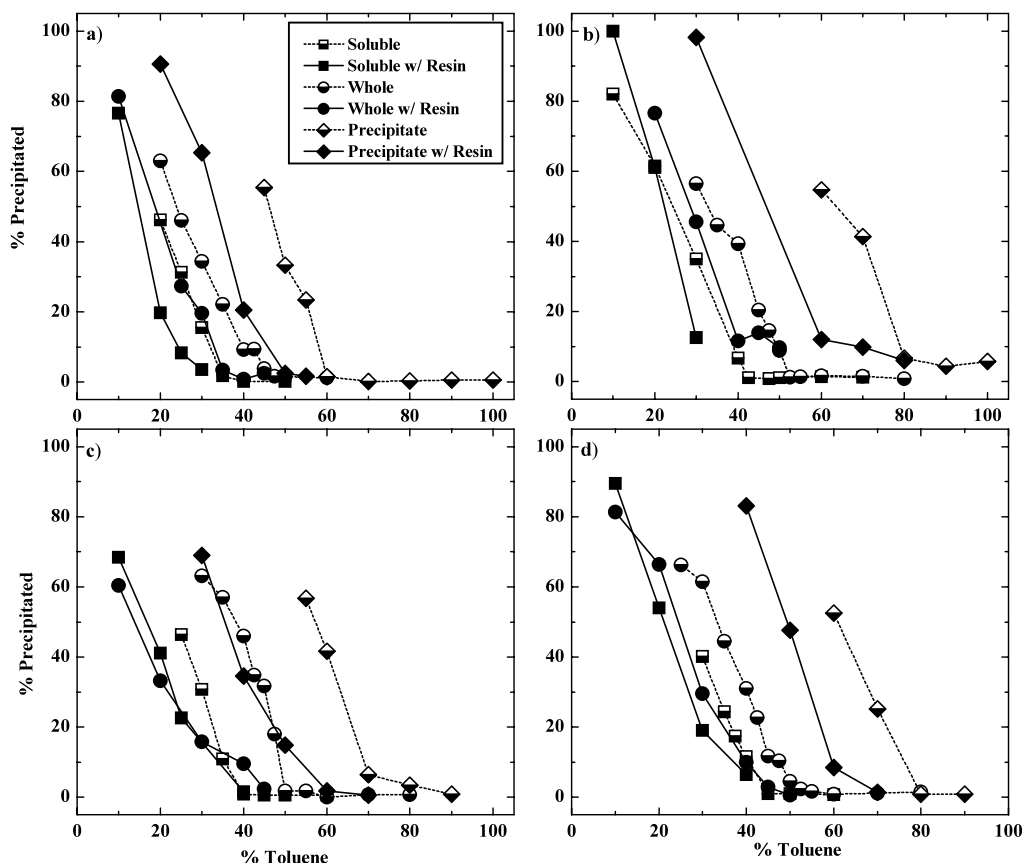


Fig. 2. Solubility of 0.75% (w/v) Whole asphaltenes and their more and less soluble subfractions in heptol with and without resins. Half filled markers denote systems without resins. R/A ratio was fixed at 1:1 by mass. a) AH, b) B6, c) CS, d) HO.

weight, and aggregate size than the Whole or Soluble asphaltene fractions. Their behavior in the presence of resins should help elucidate the molecular mechanisms of solvation and aggregation.

The asphaltene solubility limit, after resin addition, was reduced as much as 10% (v/v) toluene. In the precipitated regime, resins were capable of enhancing asphaltene solubility (reducing the percentage of precipitates) between 10 and 50%. Resins appear to enhance the solubility of the more polar and aromatic Precipitate asphaltenes more so than the Soluble asphaltenes. Soluble asphaltenes are less polar and aromatic and do not respond as favorably to resin addition in highly aliphatic solvents. Of note is the considerable solvating effect of CS resins on CS Whole and

Precipitate fractions. These interactions suggest that CS resins play a significant role in asphaltene solvation in the crude oil.

Asphaltene aggregates form in solution through intermolecular  $\pi$ - $\pi$  and hydrogen bonds between asphaltene monomers. Resins reduce the tendency for asphaltene to aggregate by disrupting these intermolecular interactions. From Table 3 we see that resins contain polar heteroatoms within a mixed aromatic–aliphatic carbon matrix. Similar to asphaltene, resins are polydisperse and only average chemical properties can be measured. Polar functional groups give resins the capacity to disrupt the electron donor–acceptor interactions partly responsible for asphaltene aggregation. Resins, however, are less aromatic than asphaltene as gauged by H/C ratios between 1.31 and

1.51. Due to decreased aromaticity, their solubility in more strongly aliphatic solvents is considerably higher than asphaltenes. Aromatic moieties in resins likely solvate the fused ring portion of the asphaltenes, producing a solvated, stabilized, resin–asphaltene aggregate. The ability of resins to dissociate intermolecular asphaltene bonds results in reduced aggregate sizes.

### 3.2. SANS: asphaltenes and resins in heptol

SANS allows us to probe the effects of resins on asphaltene aggregation. In another SANS study, we found that asphaltene Precipitate fractions formed larger aggregates than the unfractionated or more soluble fractions [44]. Scattering curves were fit with Lorentzian lineshapes to determine the solute correlation lengths. Fig. 3 shows typical  $I(Q)$  versus  $Q$  neutron scattering curves for CS Whole asphaltenes with added B6 resins in 60% toluene at 25 °C. The solid lines represent the non-

linear least squares fit of the Lorentzian lineshape to the data. Based on the shape of the neutron scattering curve alone, one can readily distinguish two length scales of aggregate sizes in typical asphaltene solutions. For example, the scattering curve for CS Whole asphaltenes with no added resins in 60% toluene (Fig. 3(a)) is a superposition of a Guinier plateau at intermediate  $Q$  and an intense power law feature at low  $Q$ . The Guinier plateau region indicated scattering from soluble, non-flocculating aggregates on the order of approximately 20–100 Å. The presence of a low  $Q$  feature indicated flocculation of a portion of the soluble aggregates. The absence of a second plateau region in the lowest  $Q$  range suggests that the largest flocs had a size greater than the order of  $1/Q_{\min}$  (or  $\geq 200$  Å). The decrease in intensity of the low  $Q$  feature with increasing resin content indicated that resins were effective at dissolving the larger flocs into non-interacting aggregates. A reduction in the correlation length

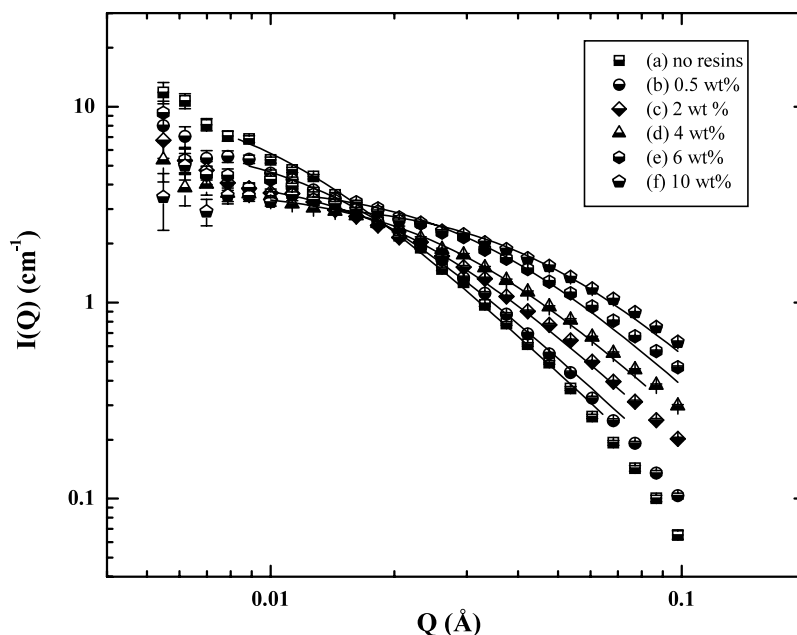


Fig. 3. SANS fits (2 mm path length) using Lorentzian lineshapes. Canadon Seco Whole asphaltenes at 25°C in 60% toluene with: (a) No Resins:  $I_0: 11.7 \pm 0.4$ ,  $\xi: 101 \pm 3$ ,  $R^2: 0.9958$ . (b) 0.5 wt.% B6 Resins:  $I_0: 6.9 \pm 0.1$ ,  $\xi: 70 \pm 1$ ,  $R^2: 0.9962$ . (c) 2 wt.% B6 Resins:  $I_0: 4.56 \pm 0.06$ ,  $\xi: 48.5 \pm 0.8$ ,  $R^2: 0.9967$ . (d) 4 wt.% B6 Resins:  $I_0: 3.80 \pm 0.03$ ,  $\xi: 36.9 \pm 0.5$ ,  $R^2: 0.9970$ . (e) 6 wt.% B6 Resins:  $I_0: 4.02 \pm 0.05$ ,  $\xi: 31.1 \pm 0.6$ ,  $R^2: 0.9940$ . (f) 10 wt.% B6 Resins:  $I_0: 3.30 \pm 0.04$ ,  $\xi: 22.5 \pm 0.4$ ,  $R^2: 0.9922$ . Note: Every 2nd data point plotted above  $Q = 0.006$ . Units of  $I$ . and  $\xi$  are  $\text{cm}^{-1} \text{Å}$  respectively.

from 101 Å (no resins) to 23 Å (10% resin) indicated that resins were also effective at solubilizing the individual asphaltene aggregates.

One trivial explanation for the decrease in SANS scattering intensity with increasing resin content is the notion that resins themselves form small aggregates similar to asphaltenes. Upon mixing the asphaltene aggregates with an increasing number of smaller resin aggregates the average particle size is expected to decrease. While resin aggregation is certainly a plausible explanation for reduced correlation lengths, asphaltene–resin interaction in solution cannot be fully discounted. The solubility studies discussed previously have shown that resins play a role in enhancing asphaltene solubility in solution. We will also show that resins are capable of modifying the surface-activity of asphaltenes, thus affecting their ability to stabilize emulsions. The resins used in this study were incapable of forming stable emulsions at any concentration or solvent condition.

Results from both the solubility and emulsion studies suggest that some interactions with resins modify the asphaltene aggregates to some extent. Bardon et al. compared the scattering curve of an asphaltene–resin mixture to the sum of the scattering intensities from pure asphaltenes and pure resins [47]. Since the sum of the individual scatterers was larger than the scattering by the mixture, they concluded that asphaltenes were solvated by resins. Furthermore, they assumed the pure asphaltene scattering intensity was the difference between the mixed asphaltene–resin and pure resin (same concentration) scattering patterns. The correlation lengths reported in this study were calculated using scattering curves from the mixed asphaltene–resin solutions, assuming that the scattering from resin-only aggregates is negligible.

The effect of resins from B6 and AH crude oils on asphaltene aggregation is shown in Fig. 4. B6 Whole asphaltenes in pure toluene and 60% (v/v) toluene in heptol were combined with AH and B6 resins at 80°C. As shown in the figure, correlation lengths of B6 Whole asphaltenes solvated by resins in pure toluene were identical with either AH or B6 resins. In the mixed solvent, AH resins may solubilize B6 asphaltenes slightly more effectively

than B6 resins. Above a 4:1 R/A ratio, the correlation lengths obtained for the asphaltene–resin systems were within 10%, regardless of the resin type. This suggests that resins from different sources may be approximately equal in effectiveness at solvating asphaltenic aggregates. Modest differences in resin aromaticity and polarity (see Table 3) are secondary to differences in asphaltene chemistry and solvent conditions for dictating aggregate size in crude oil systems. The aggregation behavior of B6 Whole asphaltene–resin solutions shown in Fig. 4 is typical of the other Whole asphaltenes as well. In the absence of resins, Whole asphaltene correlation lengths followed the trend: CS > B6 > HO > AH. Resin addition was effective at disrupting the intermolecular bonding and aggregation of each asphaltene to a similar extent. The greatest decrease in aggregate size occurred between 0.5 and 2:1 R/A suggesting resins strongly solvate asphaltenes at ratios close to those found in crude oil (Table 1). As the R/A ratio approached 10:1 the Whole asphaltene correlation lengths neared a common value of approximately 11–14 Å, suggesting this may be close to a solvated monomer or irreducible oligomer.

In less aromatic solvents, asphaltenes form larger aggregates due to solvent–solute incompatibility. Heptane–toluene mixtures of increasing aliphaticity solvent possess a lower degree of  $\pi$ -bond solvating capability and polarity than a pure toluene solvent. As a result, asphaltenes without resins in 60% (v/v) toluene have larger correlation lengths than in pure toluene. For example, B6 Whole asphaltenic aggregates have correlation lengths of 79 Å at a toluene volume fraction of 0.6 as compared with 43 Å in pure toluene. However, at a R/A ratio of 10:1 the B6 Whole correlation length appears to plateau at similar values ( $\sim$ 14–18 Å) regardless of the solvent aromaticity. This indicates that high resin concentrations are apparently more effective at reducing aggregate size than solvent alone. This comes as no surprise since resins are more chemically similar to asphaltenes and have been linked to asphaltene solubility in a variety of systems including crude oil.

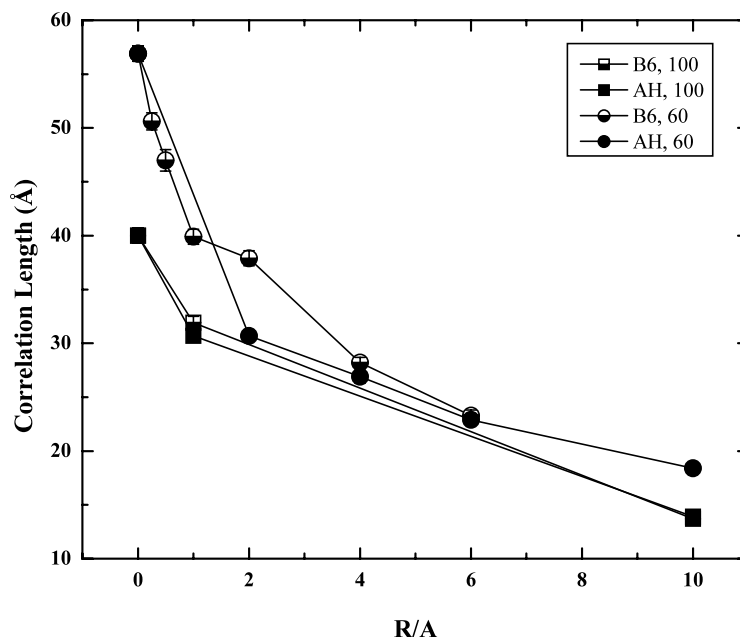


Fig. 4. Aggregate  $\xi$  of 1 wt.% B6 Whole asphaltene aggregates with AH and B6 Resins in pure toluene and 60% toluene at 80 °C determined from SANS (5 mm path length). Legend displayed as (resin type, % toluene).

### 3.3. Asphaltene–resin emulsion stability: effect of varied R/A ratio

Asphaltene emulsions were prepared in the presence of resins at R/A ratios from 0.5 to 10 and their stabilities were gauged by measuring vol. % water resolved after centrifugation. These emulsion stabilities were compared with aggregate correlation lengths determined by SANS (Figs. 5–7). As shown in Fig. 5, resin addition decreased both the aggregate correlation length and stability of emulsions formed by CS Whole asphaltenes in 60% toluene. This trend was also observed for B6 and HO Whole asphaltenes, although CS Whole asphaltenes formed much weaker emulsions than both B6 and HO Whole at similar solvent conditions. CS asphaltene aggregates were the most aromatic and least polar of the Whole asphaltenes studied. The lack of polarity and possible inability to form a network of hydrogen bonds likely reduced interfacial film strength. Resin addition up to R/A ratios of 2:1 effectively solvated the aggregates and further reduced their emulsion stabilizing ability.

Conversely, B6 Whole aggregates in 60% toluene were sufficiently surface-active (due to high polarity), even at R/A ratios approaching 5:1, to adsorb at oil–water interfaces and form emulsion-stabilizing films with 72% water resolved. Correlation lengths observed for B6 Whole asphaltenes in 60% toluene at 80 °C decreased with resin addition from 47 Å (0.5:1 R/A ratio) to 18 Å (10:1 R/A ratio). Correlation lengths observed for HO Whole asphaltenes in 60% toluene at 80 °C decreased slightly with resin addition from 38 Å (0.5:1 R/A ratio) to 14 Å (10:1 R/A ratio). Both B6 and HO Whole asphaltenes were high in polarity but HO Whole lacked the surface activity to maintain a cohesive oil–water interfacial film at R/A ratios greater than 2:1 (92% water resolved). However, emulsions formed by HO Whole asphaltenes were still more stable than those formed by CS Whole asphaltenes under similar conditions. Based on the emulsion stability results of the Whole asphaltenes, it is apparent that higher resin concentrations are needed to destabilize emulsions when asphaltenes are more polar.

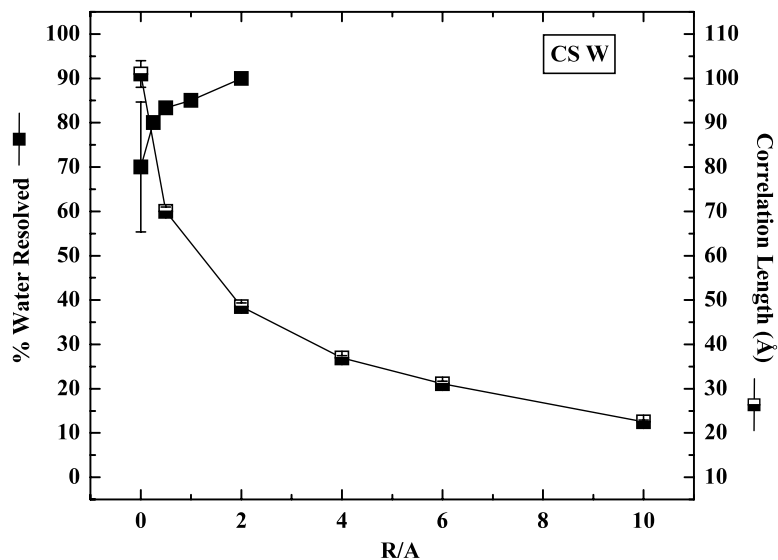


Fig. 5. Emulsion stability (% water resolved) and aggregate  $\xi$  of CS Whole asphaltenes in 60% toluene with added resins. R/A represents mass ratio of resins to asphaltenes. Emulsions tested using CS resins, 0.5 wt.% asphaltenes. SANS  $\xi$  measured at 25 °C using B6 resins, 1 wt.% asphaltenes, 2 mm path length.

B6 Precipitate emulsions prepared in pure toluene remained very stable in systems containing up to 2:1 resins (Fig. 6). This was due primarily to the high proportion of film forming species in B6 Precipitate. The fractionation process concen-

trated the most aromatic and polar asphaltenes in the Precipitate fraction and, as a result, they tended to aggregate, adsorb and consolidate into elastic films at oil–water interfaces. As the R/A ratio approached 2:1, the film forming portion of

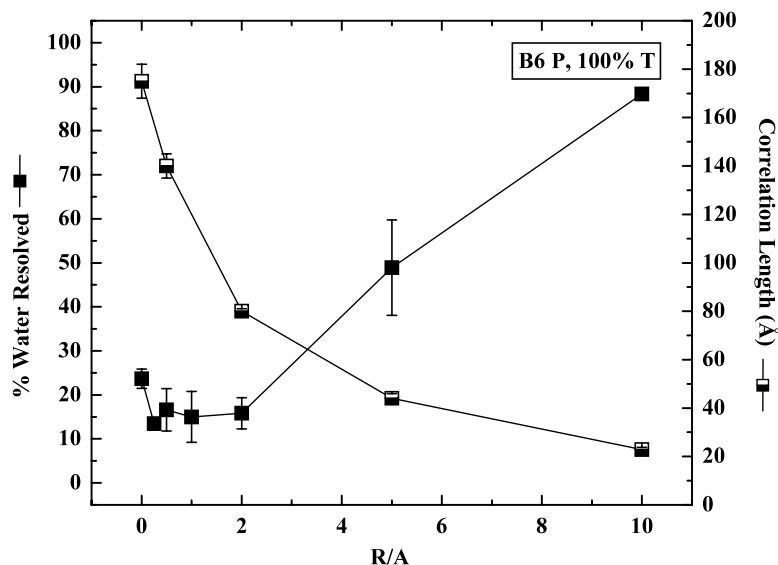


Fig. 6. Emulsion stability (% water resolved) and aggregate  $\xi$  of B6 Precipitate asphaltenes in toluene with B6 resins. Emulsions tested at 0.5 wt.% and  $\xi$  determined by SANS at 25 °C, 1 wt.% asphaltenes, and 2 mm path length.

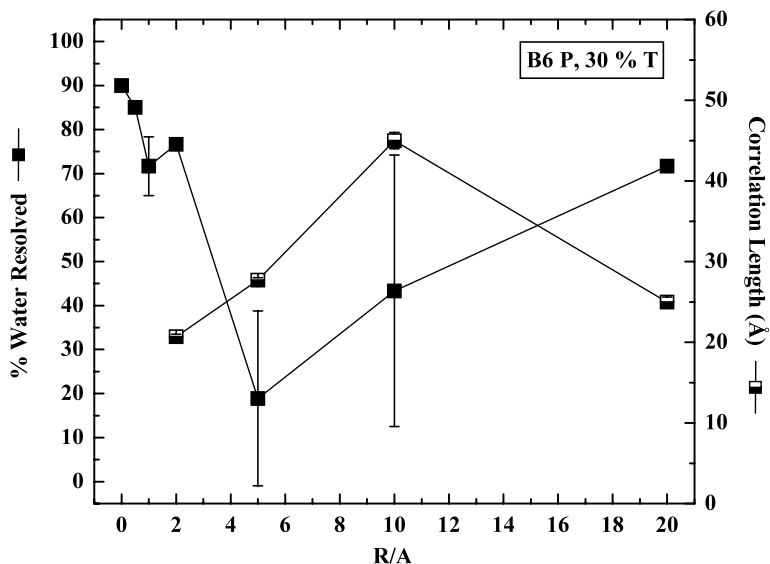


Fig. 7. Emulsion stability (% water resolved) and aggregate  $\xi$  of B6 Precipitate asphaltenes in 30% toluene with B6 resins. Emulsions tested at 0.5 wt.% and  $\xi$  determined by SANS at 25 °C, 1 wt.% asphaltenes, and 2 mm path length.

Precipitate asphaltenes were in sufficient supply to maintain nearly complete emulsion stability. The slight increase in stability from 0 to 0.25:1 R/A was likely due to enhanced asphaltene solubility and lability of the aggregates. In the absence of resins, the aggregate size may have been too large for asphaltenes to effectively cover water droplet interfaces and for w/o emulsions to achieve high stability. As the large aggregates were solvated by resins, they became more interfacially active and formed a cohesive film. Beyond 2:1 R/A the asphaltenic aggregates became increasingly soluble, less surface-active, and consequently formed weaker emulsions. The most dramatic decrease in asphaltene correlation length occurred between R/A ratios of 0.5 and 2. A minimum aggregate size was approached above 2:1 R/A and the asphaltenes were sufficiently solvated that they lost their interfacial activity.

B6 Precipitate asphaltenes were beyond the limit of solubility in 30% toluene and the emulsions prepared without resins were not particularly stable (Fig. 7). The increase in correlation length with addition of resins to a R/A ratio of 10:1 indicated that resins facilitated the dissolution of the insoluble asphaltenes. As more interfacially active material was dissolved, the emulsion stability

increased. The maximum in correlation length did not coincide with the maximum in emulsion stability, perhaps because different initial asphaltene concentrations were used for the SANS and emulsions experiments. The emulsions were tested at an asphaltene concentration of 0.5 wt.% and SANS experiments were performed at 1 wt.%. Fewer resins were needed to dissolve asphaltenes at the lower concentration, thus the maximum in emulsion stability was shifted to a R/A ratio of 5:1. At R/A of 20:1, the additional resins solvated and dissociated the asphaltenic aggregates rendering them less surface-active, and reducing the emulsion stability.

Similar trends in aggregate size and emulsion stability were observed for CS Precipitate asphaltenes in pure toluene and in 50% toluene. In pure toluene, correlation lengths increased from 101 Å (no resins) to 128 Å (0.5:1 R/A ratio) as resin addition dissolved the insoluble species followed by a monotonic decrease with further resin addition to 26 Å (10:1 R/A ratio). CS Precipitate asphaltenes did not form particularly stable emulsions in pure toluene and the addition of resins had a modest effect on emulsion stability. As expected, CS Precipitate asphaltenes were also partially insoluble in 50% toluene and the addition of resins

up to a R/A ratio of 2:1 aided the dissolution of the insoluble species. Correlation lengths observed for CS Precipitate in 50% toluene increased from 98 Å (0.5:1 R/A ratio) to 108 Å (2:1 R/A ratio) followed by a decrease to 31 Å (10:1 R/A ratio). As more interfacially active material was dissolved, the emulsion stability increased markedly from 52% water resolved (no resins) to 25% water resolved (5:1 R/A ratio).

#### 3.4. Asphaltene (Soluble, Whole, Precipitate)–resin emulsion stability

The stability of emulsions prepared with AH Whole and its fractions at several heptol ratios are shown in Fig. 8(a–c). As with the previous experiments, the asphaltene concentration was 0.37% (w/v), or equivalently 0.5% (w/w), and the resin–asphaltene ratio was varied. The volume fractions of toluene were chosen such that the asphaltenes were either above or below their solubility limits. AH Soluble asphaltenes in 60% toluene formed weak emulsions that became increasingly unstable as resin concentration increased (Fig. 8(a)). AH Soluble asphaltenes in 30% toluene were partially precipitated. Resin addition initially solvated the flocculated aggregates at R/A ratios of 0.25 and 0.5 resulting in enhanced emulsion stability. Further solvation by resins completely destabilized the emulsions at a R/A ratio of 2. AH Whole asphaltenes formed emulsions in 55% toluene with nearly 50% water resolved (Fig. 8(b)). In the insoluble regime, (30% toluene) the emulsions formed were initially weaker due to non-surface-active, flocculated asphaltenic aggregates. Resin addition up to 0.5:1 R/A increased the emulsion stability as insolubles were dissolved into solution. At higher R/A ratios, the 30% toluene system became highly solvated and emulsions were destabilized. Much the same effect was seen with AH Precipitate asphaltenes (Fig. 8(c)) where the emulsions containing the most soluble asphaltenes became unstable while partially insoluble systems actually formed stronger emulsions.

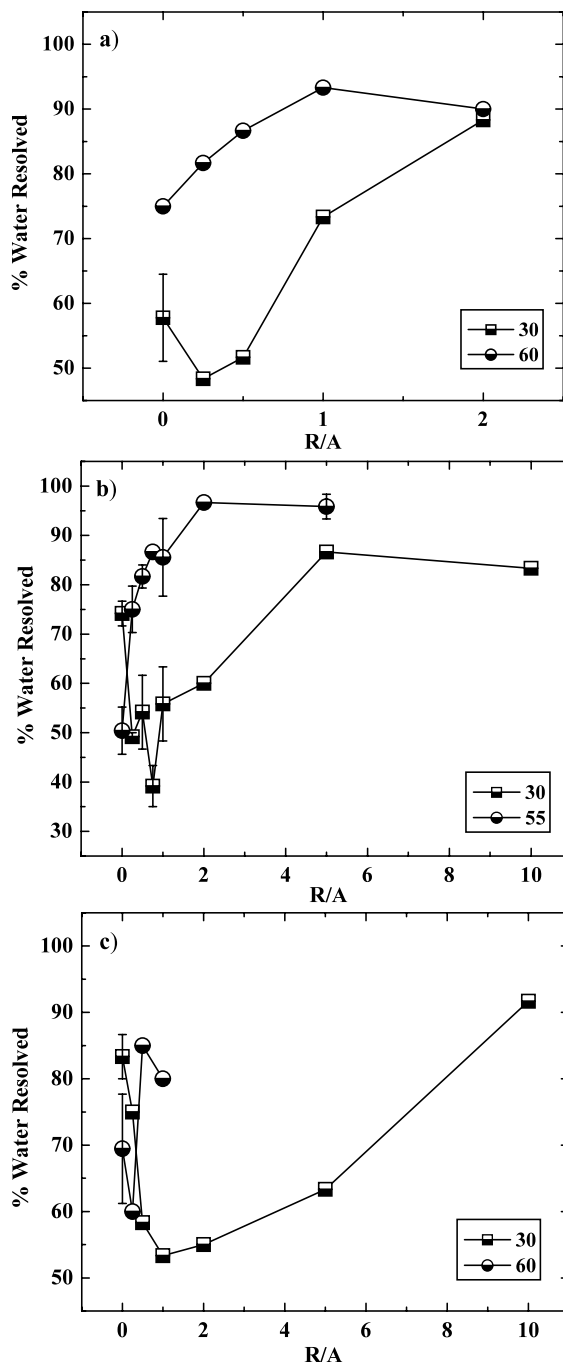


Fig. 8. Emulsion stability (% water resolved) of AH asphaltenes in heptol with AH resins. Emulsions tested at 0.5 wt.%, 25 °C. (a) Soluble: 30, 60% toluene. (b) Whole: 30, 55% toluene. (c) Precipitate: 30, 60% toluene.

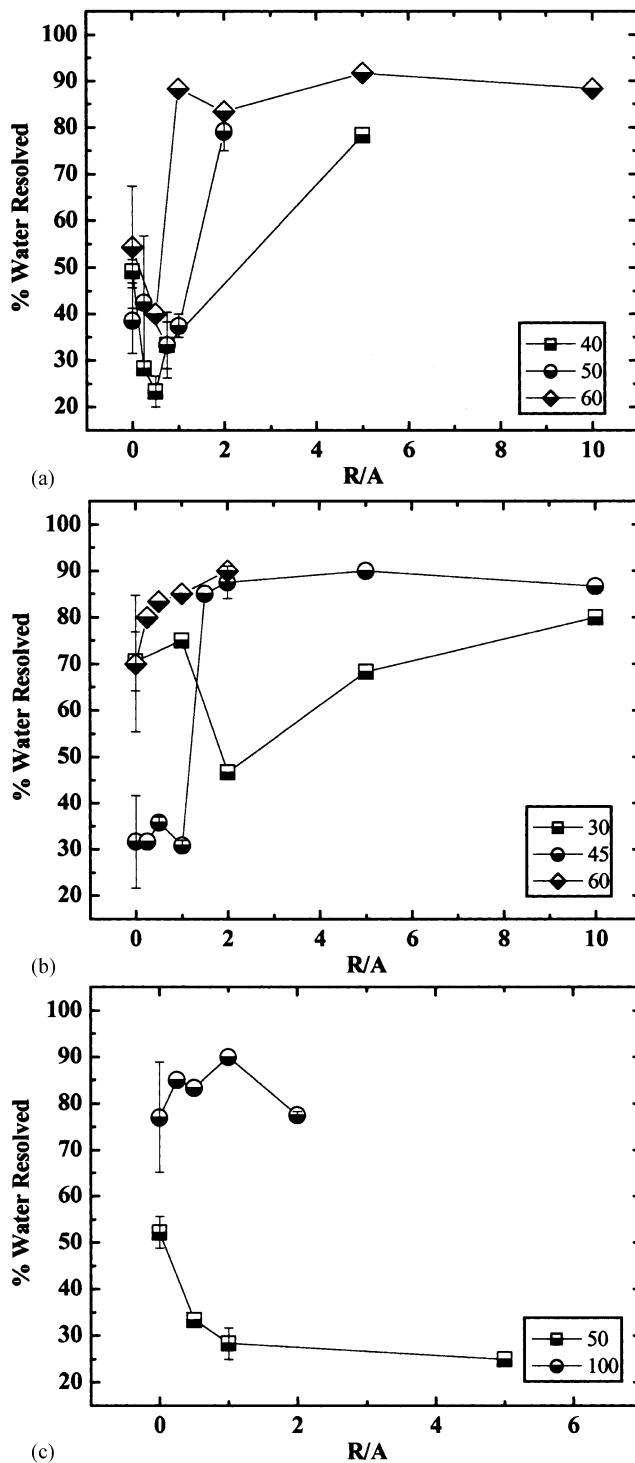


Fig. 9. Emulsion stability (% water resolved) of CS asphaltenes in heptol with CS resins. Emulsions tested at 0.5 wt.%, 25 °C. (a) Soluble: 40, 50, 60% toluene. (b) Whole: 30, 45, 60% toluene. (c) Precipitate: 50, 100% toluene.

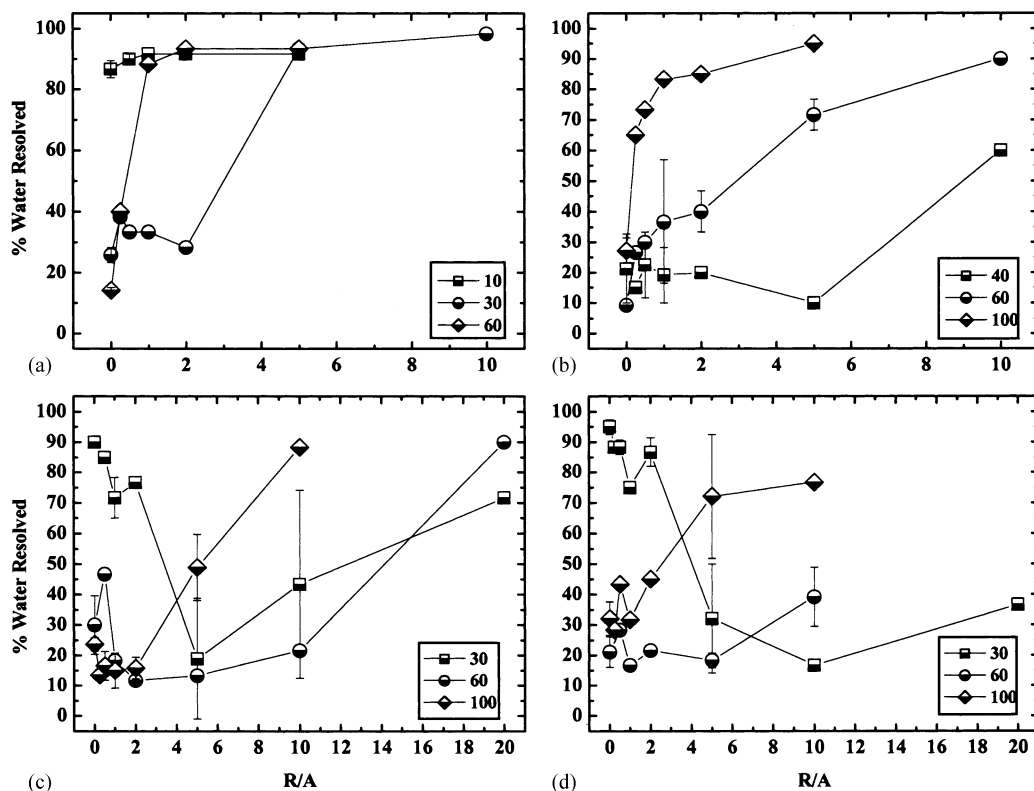


Fig. 10. Emulsion stability (vol.% water resolved) of B6 asphaltenes in heptol with B6 resins. Emulsions tested at 0.5 wt.%, 25 °C. (a) B6 Soluble: 10, 30, 60% toluene. (b) B6 Whole: 40, 60, 100% toluene. (c) B6 Precipitate: 30, 60, 100% toluene. (d) HO Precipitate: 30, 60, 100% toluene.

The emulsions formed by CS Whole asphaltenes and its more and less soluble asphaltene fractions were typically unstable. In the soluble regime, the ability of each asphaltene to form stable emulsions decreased with resin addition (Fig. 9(a–c)). The emulsion stability of CS Soluble at 40% toluene appeared to increase slightly up to an R/A of 0.5:1 followed by a decrease. CS Whole asphaltenes formed unstable emulsions beyond an R/A of 1:1 due to resin solvation. The behavior of partially insoluble CS Precipitate at 50% toluene suggests that resins were capable of a modest enhancement of emulsion stability. Even when the systems were rendered more soluble with resins, emulsion stability did not increase appreciably. High aromaticity, as suggested by low H/C ratios, likely caused the formation of large aggregates through  $\pi$ – $\pi$  interactions between asphaltene monomers and reduced aggregate lability. These properties suggest

that CS asphaltenes are inherently weak emulsifiers possibly due to large aggregate formation, low polarity and an inability to form hydrogen bonds.

Unlike the weak emulsions formed by AH and CS asphaltenes over a wide range of solvent conditions, B6 and HO asphaltene-stabilized emulsions were considerably stronger. The effects of resins on emulsion stability in the soluble and insoluble regimes are quite apparent. In Fig. 10(a), resins are shown to destabilize emulsions in the soluble regime of B6 Soluble. In the insoluble regime (30% toluene), emulsion stability is reduced only after reaching a 5:1 R/A ratio. Resins initially dissolved precipitated asphaltenes and rendered them interfacially active until the system became too soluble and the driving force for film formation disappeared. In a highly aliphatic solvent (10% toluene:90% heptane) B6 Soluble asphaltenes

did not form stable emulsions even with an R/A of 5:1.

B6 Whole asphaltenes were studied at three solvent conditions in the presence of resins (Fig. 10(b)). B6 Whole asphaltenes were completely soluble at both 60 and 100% toluene. B6 Whole asphaltenes were very soluble in pure toluene but still formed stable emulsions up to a R/A of 0.25:1. Beyond this point the emulsion stability rapidly decreased as a result of enhanced solubility. At 60% toluene, B6 Whole asphaltenes approached their limit of solubility in solution and, consequently, formed larger aggregates and stronger emulsions than observed in pure toluene. As discussed in another paper [44], aggregate size was observed to increase with decreasing solvent aromaticity up to the asphaltene solubility limit as the soluble asphaltenes attempted to minimize interactions with the increasingly aliphatic solvent. As shown in Fig. 10(b), the proximity to the solubility limit also corresponds to a maximum in emulsion stability. Emulsions of B6 Whole asphaltenes in 60% toluene eventually became unstable at a 10:1 R/A ratio, while a R/A ratio of 5:1 was needed to completely destabilize emulsions in pure toluene. Solutions containing a fraction of insoluble asphaltenes (40% toluene) were also able to form very stable emulsions up to a R/A ratio of 5:1. The dissolution of these insoluble asphaltenes facilitated strong interfacial film formation up to  $R/A > 10$ , at which point the asphaltenes were so strongly solvated by resins that they ceased to be effectively surface-active.

B6 Precipitate asphaltenes were appreciably insoluble at both 30 and 60% toluene but soluble in pure toluene. B6 Precipitate formed stable emulsions in 60 and 100% toluene; however, at 30% toluene, B6 Precipitate asphaltenes were not sufficiently soluble to stabilize emulsions (Fig. 10(c)). The effect of adding resins at 30% toluene was to effectively dissolve the insoluble asphaltenes and form strongly stable emulsions above a R/A of 5:1. Even at 20:1 R/A, there still existed a sufficient supply of film forming material to form relatively stable emulsions, a remarkable observation. This level of solubility is quite high and suggests that B6 Precipitate asphaltenes have unique molecular structures that allow them to

stabilize emulsions in the presence of large concentrations of strongly solvating resins. In particular, a balance between aromaticity and hydrogen bonding capacity must exist to allow stability in both pure toluene with no resins (high aromaticity, low polarity) and in highly aliphatic solvents with substantial resin content (low aromaticity, high polarity).

The effectiveness of resins at solubilizing asphaltenes surely depends on asphaltene and resin chemical composition and on the supporting aliphatic and aromatic solvent. B6 Whole asphaltenes formed stable emulsions at 40% toluene without resins but were only 60% soluble (Fig. 2). The amount of precipitated material decreased below 10% at an R/A of 1:1. Above this resin content, the asphaltenes were soluble and formed stable emulsions up to R/A of 5:1. Further solvation by addition of resins eventually destabilized the emulsions. At 30% toluene, B6 Precipitate asphaltenes did not form stable emulsions. Apparently, either the amount of soluble material was insufficient and/or the soluble material was in aggregates of too large a size to effectively cover water droplet surfaces. Emulsion stability increased slightly by adding resins of equal mass ratio to asphaltenes. Solubility measurements indicated that the asphaltenes were nearly insoluble at these conditions. However, at an R/A of 5:1, B6 Precipitate solubility increased from essentially insoluble to 55% soluble and emulsion stability reached a maximum. Further solvation with resins did not enhance gravimetric solubility, but emulsion stability decreased substantially.

HO Whole and its more and less soluble fractions behaved in a very similar fashion to B6 asphaltenes; however, HO Precipitate asphaltenes were observed to form even stronger emulsions than B6 Precipitate fractions (Fig. 10(d)). HO Precipitate asphaltenes were solubilized with resins at 30% toluene and formed stable emulsions up to R/A ratios of 20:1. Again, in the regime in which HO Precipitate asphaltenes were soluble, the addition of resins led to emulsion destabilization.

The power of resins to solvate asphaltenes of varied chemical composition is evident from SANS, solubility, and emulsion stability measurements. In addition, the ability to dissolve insoluble

asphaltenes and render them capable of emulsion stabilization is remarkable. However, this resin–asphaltene interaction appears to act primarily with HO and B6 Precipitate, and CS to a lesser degree, and must be linked significantly to the molecular structure of these asphaltenes. HO and B6 Precipitate fractions have the highest polarity of any of the fractions previously prepared (see Table 2). The H/C ratio of these fractions is also lower than B6 or HO Whole but not as low as AH or CS asphaltenes, indicating a moderate level of aromaticity. These chemical properties suggest that aggregation and film formation may be driven more so by polar heteroatom interactions such as hydrogen bonding than by  $\pi$ – $\pi$  bonding between asphaltenic aromatic moieties. AH and CS asphaltenes contain low concentrations of polar nitrogen and likely aggregate via aromatic stacking. Without sufficient proton donor–acceptor sites, the asphaltenes cannot adsorb and form a cohesive film at the oil–water interface.

#### 4. Conclusions

In this study, resins isolated by SARA fractionation had a strong solvating effect on asphaltenes and their more and less soluble subfractions—so-called “Soluble” and “Precipitate” asphaltenes. At an R/A ratio of 1:1, the toluene concentration at which asphaltenes began to precipitate in heptol was reduced by as much as 10%. The sizes of asphaltenic aggregates, as gauged by correlation lengths from neutron scattering, were observed to decrease significantly upon addition of resins. At room temperature, the correlation lengths of Whole asphaltenes approached a value of approximately 14–18 Å at high resin concentrations (R/A of 10:1) regardless of asphaltene, resin type, or % toluene (in the soluble regime). Furthermore, the greatest decreases in aggregate size occurred at conditions found in typical crude oils (i.e. R/A ratios between 0.5 and 2:1). It is not known to what extent the aggregates can be dissociated by resin addition. The presumed minimum would be a single asphaltene monomer solvated completely by resins. In the portion of the phase diagram in which asphaltenes were insoluble, aggregate sizes

increased with resin addition up to the solubility limit as the more polar, insoluble asphaltenes were dissolved into solution. Once the insolubles were dissolved, additional resins solvated the largest of the soluble aggregates as observed by a decrease in the correlation length.

Asphaltene stabilized emulsions were susceptible to the effects of resin solvation. Soluble asphaltenes typically formed the weakest emulsions because the aggregates were small, well solvated, less aromatic, and less polar than the Whole and Precipitate fractions, and consequently, less interfacially active. Soluble and Whole asphaltenes at toluene concentrations in the insoluble regime could be solvated by resin addition to produce slightly more stable emulsions. Resins completely destabilized emulsions of Whole and Soluble asphaltenes in the portion of phase space at which these asphaltenes were soluble at a R/A of 2:1, except in the case of B6 Whole, which formed stable emulsions up to a R/A of 10:1.

AH and CS Precipitate asphaltenes were poor emulsion formers without resins and their emulsions were only modestly more stable with resins. Their lack of polarity, even when solvated to become more labile, prevented them from interacting strongly at oil–water interfaces. B6 and HO Precipitate, however, formed very stable emulsions in their soluble regime that were resistant to the solvating effects of resins. Both approached complete instability near a R/A of 10:1. At 60% toluene B6 and HO Precipitate asphaltenes were partially insoluble but formed very stable emulsions due to their highly polar and H-bonding nature. Resins added to these systems dissolved the insoluble asphaltenic flocs, rendering them interfacially active. Once B6 Precipitate asphaltenes were solubilized, emulsions remained stable even at a R/A of 20:1. In highly aliphatic solvents (30% toluene), B6 and HO Precipitate asphaltenes were largely insoluble and did not form stable emulsions. Resins were able to solvate these systems to a considerable extent and led to stable emulsions at R/A ratios of 20:1.

Comparisons between aggregate sizes and the stability of oil-in-water emulsions formed at various R/A ratios suggested that the most stable emulsions formed from soluble aggregates of

maximum size and greatest interfacial activity. These aggregates invariably formed at the limit of asphaltene solubility. Modest differences in resin aromaticity and polarity are secondary to asphaltene chemistry and solvent conditions for dictating aggregate size and emulsion stability in asphaltene solutions.

The remarkable ability of resins to solvate asphaltenes can be attributed to the polar and dispersive nature of the resin molecules. In highly aromatic solvents, where  $\pi$ – $\pi$  interactions between asphaltenic aggregates are largely mitigated, resins serve to further disrupt polar and hydrogen-bonding interactions within asphaltene aggregates. At low solvent aromaticity, resin solvation aids to break flocs by disruption of dispersion and hydrogen bonding interactions between aggregates. For systems containing asphaltenes with high polarity and surface activity (e.g. B6 and HO Whole and Precipitate), resin solvation is sometimes insufficient to induce complete emulsion destabilization. Weak emulsion formers and Soluble asphaltenes possessing a lower polarity and aromaticity are easily destabilized in the presence of resins. Aggregation and film formation in petroleum fluids are likely driven by polar heteroatom interactions, such as hydrogen bonding. The most polar asphaltenes, typically concentrated in the least soluble fraction, require the largest concentration of resins to completely destabilize asphaltene emulsions and likely cause many petroleum production problems such as pipeline deposition and water-in-crude oil emulsion stabilization.

### Acknowledgements

This work was supported by grants from the National Science Foundation (CTS-981727), PERF (97-07), and shared consortium funding from ExxonMobil, Ondeo-Nalco Energy Systems, Shell Oil Company and Texaco. Special thanks go to George Blankenship and Semaj McIver who assisted with the experimental work. We would like to thank Eric Sirota of ExxonMobil Corporate Research for acquiring the SANS beam time at NIST and Min Lin for his assistance on the NG-7 and NG-1 beamlines. We are grateful to the

Department of Energy, Argonne National Laboratory, and particularly to Pappannan Thiagarajan and Denis Wozniak for their assistance on the SAND instrument. We also want to thank Marit-Helen Ese and Jihong Tong for helping with the SANS data collection.

### References

- [1] S.A. Berridge, M.T. Thew, A.G. Loriston-Clarke, *J. I. Petrol.* 54 (1968) 333.
- [2] C.M. Blair, *Chem. Ind.* 20 (1960) 538.
- [3] F.J. Nellensteyn, *J. I. Petrol. Technol.* 10 (1924) 311.
- [4] J.P. Pfeiffer, R.N.J. Saal, *J. Phys. Chem.* 44 (1940) 139.
- [5] A.S.C. Lawrence, W. Killner, *J. I. Petrol.* 34 (1948) 281.
- [6] M.O. Denekas, F.T. Carlson, J.W. Moore, C.G. Dodd, *Ind. Eng. Chem.* 43 (1951) 1165.
- [7] C.G. Dodd, *J. Phys. Chem.* 64 (1960) 544.
- [8] H. Neumann, *Petrochemie* 18 (1965) 776.
- [9] O.K. Kimbler, R.L. Reed, I.H. Silberberg, *Soc. Petrol. Eng. J.* 6 (1966) 153.
- [10] J.E. Strassner, *J. Petrol. Technol.* 20 (1968) 303.
- [11] G.D.M. Mackay, A.Y. McLean, O.J. Betancourt, B.D. Johnson, *J. I. Petrol.* 59 (1973) 164.
- [12] R.J.R. Cairns, D.M. Grist, E.L. Neustadter, in: A.L. Smith (Ed.), *Theory and Practice of Emulsion Technology*, Academic Press, Brunel University, 1974, p. 135.
- [13] J.J. Oren, G.D.M. MacKay, *Fuel* 56 (1977) 382.
- [14] T.J. Jones, E.L. Neustadter, K.P. Whittingham, *J. Can. Petrol. Technol.* 17 (1978) 100.
- [15] A.L. Bridie, T.T. Wanders, W. Zegveld, H.B. van der Heijde, *Mar. Pollut. Bull.* 11 (1980) 343.
- [16] S.E. Taylor, *Chem. Ind.* 20 (1992) 770.
- [17] C.S. Shetty, A.D. Nikolov, D.T. Wasan, *J. Disper. Sci. Technol.* 13 (1992) 121.
- [18] D.L. Mitchell, J.G. Speight, *Fuel* 52 (1973) 149.
- [19] T.F. Yen, J.G. Erdman, S.S. Pollack, *Anal. Chem.* 33 (1961) 1587.
- [20] R.V. Barbour, J.C. Petersen, *Anal. Chem.* 46 (1974) 273.
- [21] M.M. Boduszynski, J.F. McKay, D.R. Latham, *Proc. Assoc. Asphalt Paving Technol.* 49 (1980) 123.
- [22] T. Ignasiak, O.P. Strausz, D.S. Montgomery, *Fuel* 56 (1977) 359.
- [23] S.E. Moschopedis, J.G. Speight, *Fuel* 55 (1976) 187.
- [24] J.C. Petersen, *Fuel* 46 (1967) 295.
- [25] M.M.H. Al-Jarrah, A.H. Al-Dujaili, *Fuel Sci. Technol. Int.* 7 (1989) 69.
- [26] S. Acevedo, B. Mendez, A. Rojas, I. Layrisse, H. Rivas, *Fuel* 64 (1985) 1741.
- [27] M.M. Boduszynski, *Energy Fuels* 2 (1988) 597.
- [28] I.A. Wiehe, K.S. Liang, *Fluid Phase Equilib.* 117 (1996) 201.
- [29] J.F. McKay, P.J. Amend, T.E. Cogswell, P.M. Harnsberger, R.B. Erikson, D.R. Latham, in: P.C. Uden, S. Siggia

- (Eds.), Analytical Chemistry of Liquid Fuel Sources: Tar Sands, Oil Shale, Coal, and Petroleum, vol. 170, American Chemical Society, Washington, 1979, p. 128.
- [30] S.I. Andersen, A. Keul, E. Stenby, *Petrol. Sci. Technol.* 15 (1997) 611.
- [31] H.W. Yarranton, J.H. Masliyah, *AIChE J.* 42 (1996) 3533.
- [32] H.W. Yarranton, H. Alboudwarej, R. Jakher, *Ind. Eng. Chem. Res.* 39 (2000) 2916.
- [33] P. Herzog, D. Tchoubar, D. Espinat, *Fuel* 67 (1988) 245.
- [34] J.C. Ravey, G. Ducouret, D. Espinat, *Fuel* 67 (1988) 1560.
- [35] R.E. Overfield, E.Y. Sheu, S.K. Sinha, K.S. Liang, *Fuel Sci. Technol. Int.* 7 (1989) 611.
- [36] E.Y. Sheu, D.A. Storm, M.M.D. Tar, *J. Non-Cryst. Solids* 131–133 (1991) 341.
- [37] D. Espinat, J.C. Ravey, V. Guille, J. Lambard, T. Zemb, J.P. Cotton, *J. Phys. IV* 3 (1993) 181.
- [38] P. Thiyagarajan, J.E. Hunt, R.E. Winans, K.B. Anderson, J.T. Miller, *Energy Fuels* 9 (1995) 829.
- [39] H. Rassamdana, M. Sahimi, *AIChE J.* 42 (1996) 3318.
- [40] L. Barre, D. Espinat, E. Rosenberg, M. Scarcella, *Rev. I. Fr. Petrol.* 52 (1997) 161.
- [41] M.Y. Lin, E.B. Sirota, H. Gang, *Abstr. Pap. Am. Chem. S.* 213 (1997) 66.
- [42] E.B. Sirota, *Petrol. Sci. Technol.* 16 (1998) 415.
- [43] D. Fenistein, L. Barre, *Fuel* 80 (2001) 283.
- [44] P.M. Spiecker, K.L. Gawrys, P.K. Kilpatrick, *J. Colloids Interf. Sci.*, 2003, in press.
- [45] O.P. Strausz, P. Peng, J. Murgich, *Energy Fuels* 16 (2002) 809.
- [46] E.Y. Sheu, K.S. Liang, S.K. Sinha, R.E. Overfield, *J. Colloids Interf. Sci.* 153 (1992) 399.
- [47] C. Bardon, L. Barre, D. Espinat, V. Guille, M.H. Li, J. Lambard, J.C. Ravey, E. Rosenberg, T. Zemb, *Fuel Sci. Technol. Int.* 14 (1996) 203.
- [48] J.C. Ravey, D. Espinat, *Prog. Coll. Pol. Sci.* 81 (1990) 127.
- [49] P.M. Spiecker, Ph.D. Thesis. North Carolina State University, 2001 .
- [50] M. van der Waarden, *Kolloid Z. Z. Polym.* 156 (1958) 116.
- [51] R. Miller, *Anal. Chem.* 54 (1982) 1742.
- [52] J.G. Reynolds, *Fuel Sci. Technol. Int.* 5 (1987) 593.
- [53] M.F. Ali, A. Bukhari, M.U. Hasan, *Fuel Sci. Technol. Int.* 7 (1989) 1179.
- [54] M. Alula, M. Diack, R. Gruber, G. Kirsch, J.C. Wilhelm, D. Cagniant, *Fuel* 68 (1989) 1330.
- [55] W.R. Middleton, *Anal. Chem.* 39 (1967) 1839.
- [56] J.G. Reynolds, W.R. Biggs, *Fuel Sci. Technol. Int.* 4 (1986) 749.
- [57] L.X. Nghiem, M.S. Hassam, R. Nutakki, A.E.D. George, *S. Petrol. Eng.* 5 (1993) 375.
- [58] S.I. Andersen, K.S. Birdi, *J. Colloid Interf. Sci.* 142 (1991) 497.
- [59] J. Murgich, J.A. Abanero, O.P. Strausz, *Energy Fuels* 13 (1999) 278.
- [60] J. Murgich, O.P. Strausz, *Petrol. Sci. Technol.* 19 (2001) 231.
- [61] J.D. McLean, P.K. Kilpatrick, *J. Colloid Interf. Sci.* 196 (1997) 23.
- [62] H. Fordedal, Y. Schildberg, J. Sjoblom, J.-L. Volle, *Colloids Surf. A* 106 (1996) 33.
- [63] R.A. Mohammed, A.I. Bailey, P.F. Luckham, S.E. Taylor, *Colloids Surf. A* 80 (1993) 237.
- [64] H. Fordedal, Y. Schildberg, J. Sjoblom, J.-L. Volle, *J. Colloid Interf. Sci.* 182 (1996) 117.
- [65] J.D. McLean, P.K. Kilpatrick, *J. Colloid Interf. Sci.* 189 (1997) 242.
- [66] O.V. Gafonova, H.W. Yarranton, *J. Colloid Interf. Sci.* 241 (2001) 469.
- [67] J.D. McLean, P.K. Kilpatrick, *Energy Fuels* 11 (1997) 570.
- [68] P.-G. de Gennes, *Scaling Concepts in Polymer Physics*, Cornell University Press, Ithaca, 1979.